while the region $E_F^0 \leq 1$ MeV is practically excluded. This conclusion is supported also by the data analysis of the ^{240}Pu fission with emission of other light nuclei and by the analysis of the data on other fissioning nuclei.

Finally, our conclusion is that, in spite of some limitations of the methods used for analyzing the experimental data, one can state with reasonable confidence that the kinetic energy of the fragments at the moment of scission is quite high ($E_F^0 \geq$20 MeV). That means, in particular, that the statistical model of fission (which requires $E_F^0 \leq 1$ MeV) can not describe the fission process. The most preferable is the dynamic model which assumes that the fragments are formed at the barrier with the subsequent fast evolution towards the scission point without essential re-distribution of the fragments masses.

References

[1] *A.A.Vorobyov, V.T.Grachov, A.P.Komar, I.A.Kondurov, A.M.Nikitin, D.M.Seliverstov.* // Atomnaya Energiya, 1969. V.27. P.31.

[2] *A.A.Vorobyov, V.T.Grachov, I.A.Kondurov, A.M.Nikitin, D.M.Seliverstov.* // Elem. Chast. Atom. Yadra, 1972. V.2. P.941.

[3] *A.A.Vorobyov, D.M.Seliverstov, V.T.Grachov, I.A.Kondurov, A.M.Nikitin, A.I.Egorov, Yu.K.Zalite.* // Phys. Lett., 1969. V.30B. P. 332.

[4] *A.A.Vorobyov, D.M.Seliverstov, V.T.Grachov, I.A.Kondurov, A.M.Nikitin, N.N.Smirnov, Yu.K.Zalite.* // Phys. Lett., 1972. V.40B. P.102.

[5] *A.A.Vorobyov, V.T.Grachov, I.A.Kondurov, Yu.A.Miroshnichenko, A.N.Nikitin, D.M.Seliverstov, N.N.Smirnov.* // Yad. Fiz., 1974. V.20. P.461.

[6] *A.A.Vorobyov, V.T.Grachov, Yu.K.Zalite, I.A.Kondurov, A.M.Nikitin, D.M.Seliverstov.* Preprint FTI-232, Leningrad, 1969. 24p.

[7] *V.T.Grachov, Yu.I.Gusev, D.M.Seliverstov, N.N.Smirnov.* // Yad. Fiz., 1980. V.32. P.1186.

[8] *V.T.Grachov, Yu.I.Gusev, D.M.Seliverstov.* // Yad. Fiz., 1988. V.47. P.622.

[9] *Yu.I.Gusev, D.M.Seliverstov.* // Voprosy Atom. Nauki Tekhnol., Ser. Yad. Konst., 1988. V.1. P.24.

[10] *M.Ya.Borkovsky, Yu.I.Gusev, Yu.K.Zalite, D.M.Seliverstov.* Preprint LNPI-1540, Leningrad, 1989. 36p.

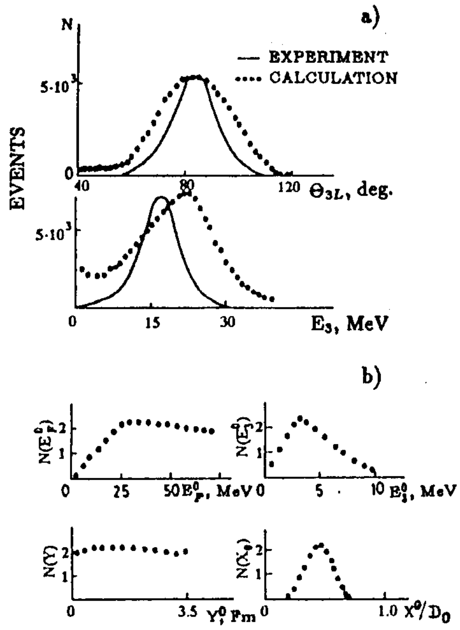

Fig. 10. Results of analysis with the uniform distributions method. ^{240}Pu fission with emission of α-particles.
a) Final energy and angular distributions of α-particles. Solid lines – experiment, dotted lines – results of calculations with the uniform initial distributions of E_F^0, E_3^0, Y^0, X^0.
b) Initial distributions of E_F^0, E_3^0, Y^0, X^0 bringing to agreement with experimental distributions of E_3 and Θ_{3L}.

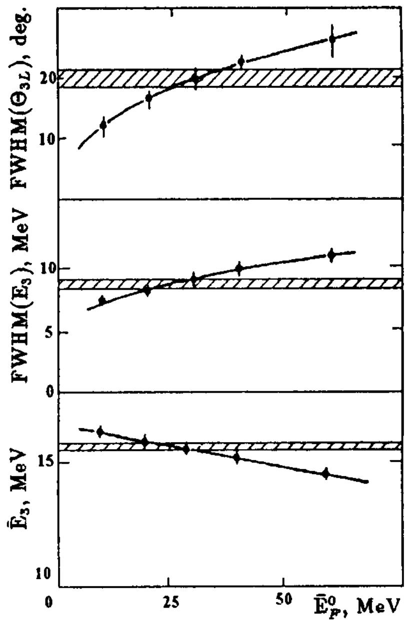

Fig. 11. Dependence of $\bar{E}_3$, FWHM(E_3), and FWHM(Θ_{3L}) on E_F^0. ^{240}Pu fission with emission of α-particles. The shaded areas are the regions allowed by the errors of the experiment.

free parameter. The X^0-distribution was a Gaussian centered in the minimum of the potential energy with FWHM(X^0/D_0) = 0.27 (this value follows from the results of the calculations shown in Fig. 10b). The initial angular Θ_{3L}^0-distribution was isotropic. The initial Y^0-distribution was uniform in the region $0 \leq Y^0 \leq Y_{max}^0$. So, in total there were 5 fitting parameters: $\bar{E}_F^0$, FWHM(E_F^0), FWHM(V_C), T, and Y_{max}^0. As an example, we present the results of analysis of the experimental data on the ^{240}Pu fission with α-particles emission. The following set of the initial conditions has been obtained from comparison with the experimental data.

E_3^0 – Maxwell distribution, T= 1.4 MeV;
E_F^0 – Gaussian distribution, $\bar{E}_F^0$ = 30 MeV, FWHM(E_F^0) = 10 MeV;
V_C – Gaussian distribution, FWHM(V_C) = 16 MeV;
X^0 – Gaussian distribution, FWHM(X^0/D_0) = 0.27 (fixed) with $\bar{X}^0$ in the minimum of potential energy;
Y^0 – uniform distribution, $0 < Y^0 < 3.5$ fm;
Θ_{3L}^0 – isotropic distribution, $0 < \Theta_{3L}^0 < 180°$.

Fig. 11 shows the calculated values of $\bar{E}_3$, FWHM(E_3), and FWHM(Θ_{3L}) as functions of E_F^0. One can see that the best agreement with the experiment is reached at E_F^0 = 30 MeV

Kinematics analysis of ternary fission

The extraction of quantitative information on the initial conditions of the fragments separation is usually accomplished by trajectory calculations of the three bodies movement in their mutual Coulomb field. The calculation starts at the moment of the nucleus neck rupture when the nuclear forces between the fragments are not acting anymore. The coordinates and the velocities of the three charged spherically symmetric bodies were assumed as the initial conditions. Then the equations of movement are solved, and the energies and the trajectories of the moving away heavy fragments and the light nucleus are determined. Some distributions of the initial conditions are generated for comparison with the experiment in a way to get the best agreement with the measured distributions. Unfortunately, in this analysis there is no strict correspondence between the final and the initial distributions. However, reliability of the initial conditions reconstruction increases with involving into the analysis more experimental distributions.

The kinematics analysis of the ^{236}U, ^{240}Pu, ^{252}Cf ternary fission was carried out at PNPI using all the information obtained in the correlation measurements with ^{3}H, ^{4}He, ^{6}He, and ^{10}Be nuclei. Two calculation methods were used differing in the way of generation and selection of the initial conditions.

Method of uniform initial distributions

In this case, the initial conditions were selected by the Monte Carlo method starting from uniform distributions in a wide range of the variables:

$$0 < E_F^0 < 70 \text{ MeV} \qquad 0 < E_3^0 < 10 \text{ MeV}$$
$$0 < Y^0 < 3.5 \text{ fm} \qquad 0 < \Theta_{3L}^0 < 180^\circ$$
$$0 < X^0/D_0 < 1.0 \qquad N(\Theta_{3L}^0) = \text{const} \times \sin\Theta_{3L}^0.$$

Here X^0 and Y^0 are the coordinates of the light nucleus along the directions parallel and perpendicular to the axis connecting the fragments centers, respectively, and D_0 is the distance between the centres of the fragments at the moment of their separation. The mass ratio $R = M_H/M_L$ and the total kinetic energy $E_T = E_F + E_3$ were fixed in each set of the calculations. The selection of simulated events was performed by filling each cell of the two-dimensional matrix $E_3 - \Theta_{3L}$ up to the level equal to that in the matrix obtained in the experiment. The events leading to overflow of any cell were rejected. As a result, the initially uniform distributions were transformed into distributions shown in Fig. 10. This figure shows the results of the analysis of the ^{240}Pu fission with α-particles emission. Already this analysis shows that the large values of the initial kinetic energy of the fragments are preferable: $E_F^0 \geq 25$ MeV. As to the region $E_F^0 \leq 1$ MeV, it appeared to be excluded by the experimental data.

Method of parametrized initial distributions

In this method, the initial conditions were represented by some properly chosen distributions with a set of fitting parameters. In particular, the E_3^0-values were distributed according to the Maxwell distribution with the temperature T used as a free parameter. The E_F^0-distribution was a Gaussian with $\bar{E}_3^0$ and FWHM(E_F^0) as free parameters. Similarly, the distribution of the initial Coulomb energy $V_C = Z_L Z_H / D_0$ was taken as a Gaussian with FWHM(V_C) as a

Table 1
Comparison of the mean masses of the fragments produced in ternary and binary fission of ^{235}U induced by thermal neutrons

Light nuclei	$\Delta\overline{M}_L^{BT}$	$\Delta\overline{M}_H^{BT}$
^{3}H	0.7 ± 0.15	1.9 ± 0.15
^{4}He	2.1 ± 0.1	1.5 ± 0.1
^{6}He	2.9 ± 0.3	2.4 ± 0.3
^{10}Be	5.2 ± 0.3	3.7 ± 0.3

Table 2
Parameters of the light nuclei angular distributions

Fission nuclei	^{3}H		^{4}He		^{6}He		^{10}Be	
	$< \Theta_{3L} >$	$\sigma(\Theta_{3L})$	$< \Theta_{3L} >$	$\sigma(\Theta_{3L})$	$< \Theta_{3L} >$	$\sigma(\Theta_{3L})$	$< \Theta_{3L} >$	$\sigma(\Theta_{3L})$
^{236}U	81.4 ± 0.5	12.6 ± 0.5	81.9 ± 0.5	8.1 ± 0.4	81.3 ± 0.4	6.8 ± 0.4	82.4 ± 0.8	4.7 ± 0.6
^{240}Pu	83.0 ± 0.6	12.2 ± 0.6	83.7 ± 0.4	8.2 ± 0.4	83.4 ± 0.9	6.8 ± 0.8	–	–
^{252}Cf	83.7 ± 0.2	12.2 ± 0.2	84.6 ± 0.2	7.7 ± 0.1	84.4 ± 0.2	6.7 ± 0.2	–	–

Note: Θ_{3L} and $\sigma(\Theta_{3l})$ are given in degrees. For ^{3}H, ^{4}He, and ^{6}He the results are given for the whole energy spectra.

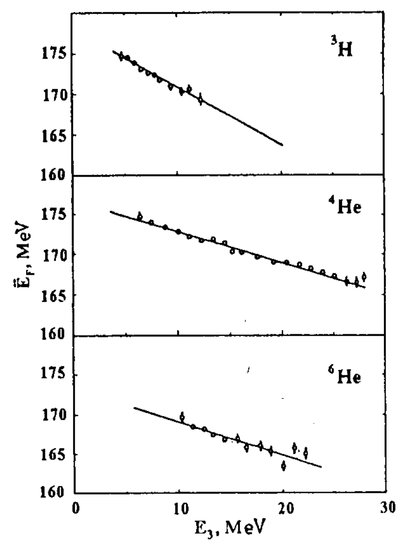

Fig. 8. Dependence of the mean kinetic energy $\overline{E}_F$ of the fission fragments on the light nuclei energy. ^{252}Cf spontaneous fission.

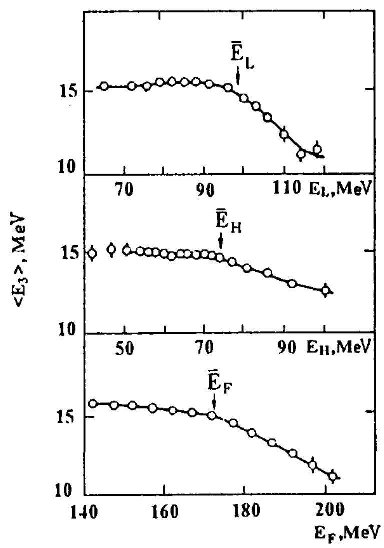

Fig. 9. Dependence of the α-particles most probable energy on kinetic energy of light fragment E_L, of heavy fragment E_H, and of both fragments E_F. ^{252}Cf spontaneous fission.

the fission followed by the emission of the even-even light nuclei both fragments participate in their formation approximately equally. In the fission accompanied by the ^{3}H emission the contribution of the heavy fragment is noticeably higher.

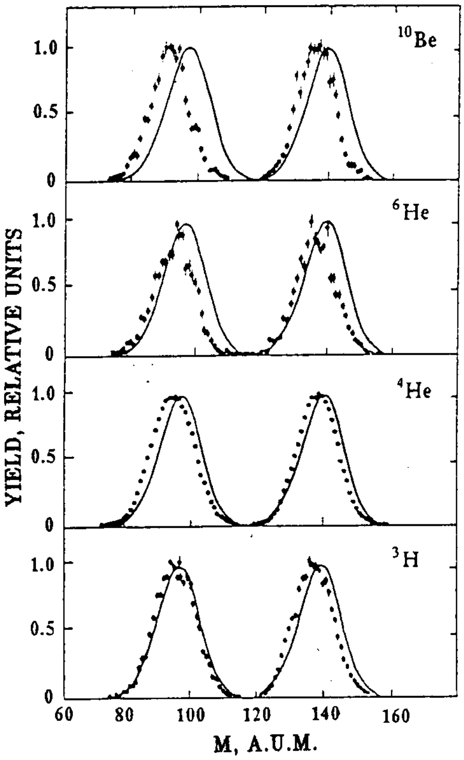

Fig. 7. Mass spectra of the fragments in ^{235}U fission induced by thermal neutrons accompanied by emission of ^{3}H, ^{4}He, ^{6}He, ^{10}Be nuclei. The curves – similar spectra for binary fission.

The correlations between the kinetic energies of the fragments and that of the light nuclei are important for understanding the ternary fission mechanism. These correlations are quantitatively characterized by the anticorrelation parameter $\beta = -d\overline{E}_F/dE_3$ usually determined from approximation of the experimental data with the linear dependence (Fig. 8). The deviation of the β values from –1 is interpreted as an indication of the high initial velocity of the fragments. Prior to our measurements, the experimental β values for α-particles were around $|\beta| = 0.4 - 0.45$. The data shown in Fig. 8 are characterized by the following β values: $\beta = -0.64 \pm 0.03$ (^{3}H), $\beta = -0.50 \pm 0.01$ (^{4}He), and $\beta = -0.38 \pm 0.03$ (^{6}He). Fig. 9 shows the correlations between the most probable energy of the α-particles and the fragments energy.

Parameters of the light nuclei angular distributions are given in Table 2. The angular distributions of ^{4}He in the uranium and californium fission fit well the world data (Grenoble, Darmstadt). The other results are obtained for the first time.

Angular characteristics are a sensitive criterion for the E_F^0 determination on the base of different model calculations. For example, Z.Fraenkel has got the value of $E_F^0 = 40$ MeV being guided mostly by the $\sigma(\Theta_{3L})$ for the α-particles from the ^{252}Cf fission. By the way, he used $\sigma(\Theta_{3L}) = 13°$ which differs significantly from the up-to-date data.

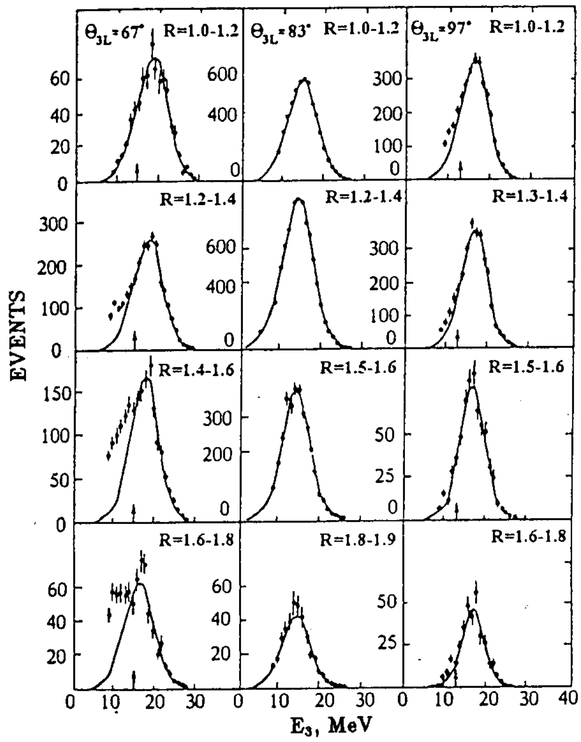

Fig. 5. Energy spectra of α-particles for different values of $R = M_H/M_L$ and Θ_{3L}. The curves are Gaussian distributions, arrows point out the lowest energies taken in the fit.

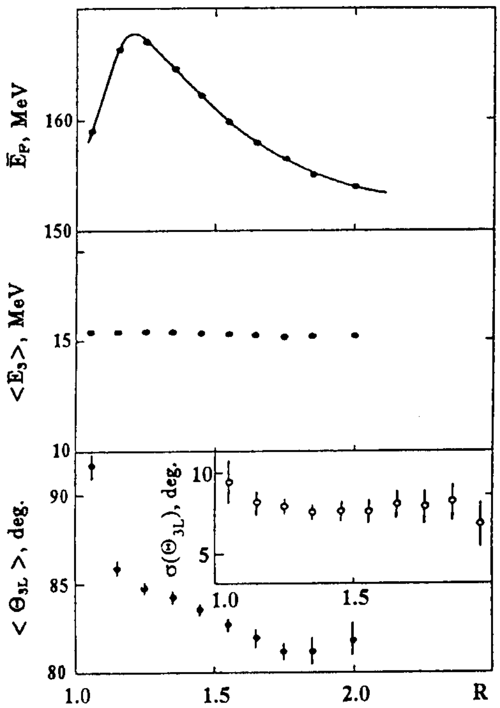

Fig. 6. $\overline{E}_F$, $< E_3 >$, $< \Theta_{3L} >$, $\sigma(\Theta_{3L})$ as functions of R for ^{239}Pu fission induced by thermal neutrons with emission of α-particles. The curve is drawn through the experimental points.

at the most probable angle ($\Theta_{3L} = 83°$) and in the direction of the heavy fragment ($\Theta_{3L} = 97°$) are little sensitive to the ratio of the fragments masses. On the contrary, for the α-particles moving in the direction of the light fragment ($\Theta_{3L} = 67°$) the shape of the spectra essentially depends on R. This fact is explained by the effect of re-scattering of the particles by the moving fragment, which leads to enrichment of the low-energy part of the spectrum. Such a decrease of the scattered particle energy is possible in case of the fast separation of the fragments. This effect is more visible in emission of heavier clusters like ^{6}He and ^{10}Be.

The dependence of the mean kinetic energy $\overline{E}_F$ of the ternary fission fragments on R (Fig. 6) follows the character of the $\overline{E}_F$ dependence on R in the binary fission and also the dependence of the total energy release Q on R. This fact was one of the main arguments in favour of identity of the two types of fission differing only in the last stage of the nuclear neck rupture.

The most probable particle energies $< E_3 >$ turned out to be non-sensitive to R (Fig. 6). This may be explained by considerable velocities of the fragments at the moment of scission neutralizing the difference in the energy release at different R values.

The mass distributions of the ternary fission fragments are similar for all studied fissioning nuclei. Fig. 7 shows an example of the fragments mass spectra of the ^{235}U fission induced by thermal neutrons. The difference in the mean masses of the light ($\Delta\overline{M}_L^{BT}$) and heavy ($\Delta\overline{M}_H^{BT}$) fragments in binary and ternary fission is given in Table 1. One can see that in

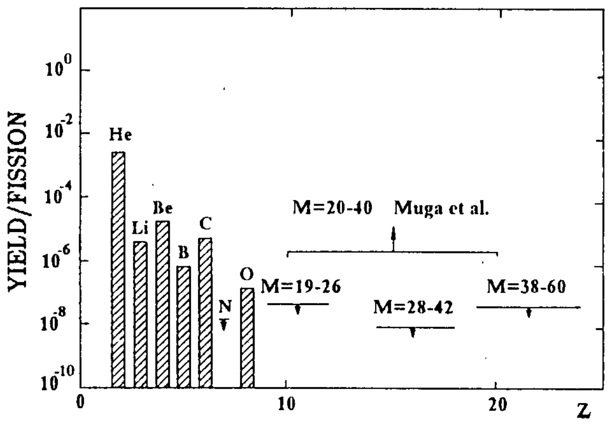

Fig. 4. Yields of light nuclei from ^{235}U fission induced by thermal neutrons. The data by M.Muga et al. is the lower limit.

10^{-8} 1/fission. In 1967, M.Muga et al. reported on discovery of the "true" ternary fission into three relatively heavy fragments on the level of 10^{-6} 1/fission (Fig. 4). Our measurements performed with significantly higher sensitivity have not confirmed these results (Fig. 4). In 1989 I.Theobald and M.Mutterer studied spontaneous fission of ^{252}Cf and they came to a similar conclusion. So one can state that the "true" ternary fission at low excitation energies does not exist, at least on the level of 10^{-8} 1/fission.

In a special experiment with an ^{235}U target, we made a search for a hypothetical nuclear-stable isotope ^{10}He [6]. Our method of nonlinear extrapolation of the neutron binding energies [6] for determination of the separation energy for one and two neutrons gave in the case of ^{10}He: $E_n = +0.6$ MeV, $E_{2n} = -1.2$ MeV. Such a small instability (–1.2 MeV) required an experimental test and motivated our experiment. We succeeded in setting the lower limit on production rate of this nucleus on a level of $< 2 \cdot 10^{-10}$ 1/fission which can be interpreted as non-existence of the nuclear-stable ^{10}He in nature.

Energy and angular distributions of light nuclei in correlation experiments

In correlation experiments, we measured the energy of the light nuclei emitted at different angles Θ_{3L} relatively to the direction of the light fragment and also the energies of the fragments E_L and E_H. In the majority of earlier experiments (K.Ge, ^{235}U, 1979, Grenoble; M.Mutterer, ^{252}Cf, 1989, Darmstadt) the third fragment was the α-particle. In our experiments, we studied the ^{233}U and ^{239}Pu fission induced by thermal neutrons as well as the spontaneous fission of ^{252}Cf with emission of ^{3}H, ^{4}He, ^{6}He, and ^{10}Be nuclei. The correlation measurements were performed with a multicounter setup consisting of a grid ionization chamber (10×10 cm^2) for measuring $\Delta E/\Delta x$ followed by a mosaic of silicon detectors for measuring the energy E_3 of the light nuclei. Also, two mosaics of silicon detectors were used for measuring the energy of the fission fragments. The precision of the Θ_{3L} determination for α-particles was $\pm 1°$ and the range of the simultaneously measured angles was $60° - 120°$. An example of the energy spectra of the α-particles from the ^{252}Cf spontaneous fission is given in Fig. 5. The complete account on our correlation measurements is published in Refs. [7–9].

The character of the α-particles spectra obtained at different Θ_{3L} and $R = M_H/M_L$ (Fig. 5) may indicate a considerable energy E_F^0. Fig. 5 demonstrates that the spectra of the α-particles measurements, while most of the other data was obtained for the first time.

Considering the energy spectra and the yields of the light nuclei (Fig. 3), one should note the independence of the most probable energies $< E_3 >$ of ^{3}H, ^{4}He, ^{6}He on Z^2/A of the fissioning nucleus. In the case of ^{10}Be, $< E_3 >$ even decreases with the increase of Z^2/A.

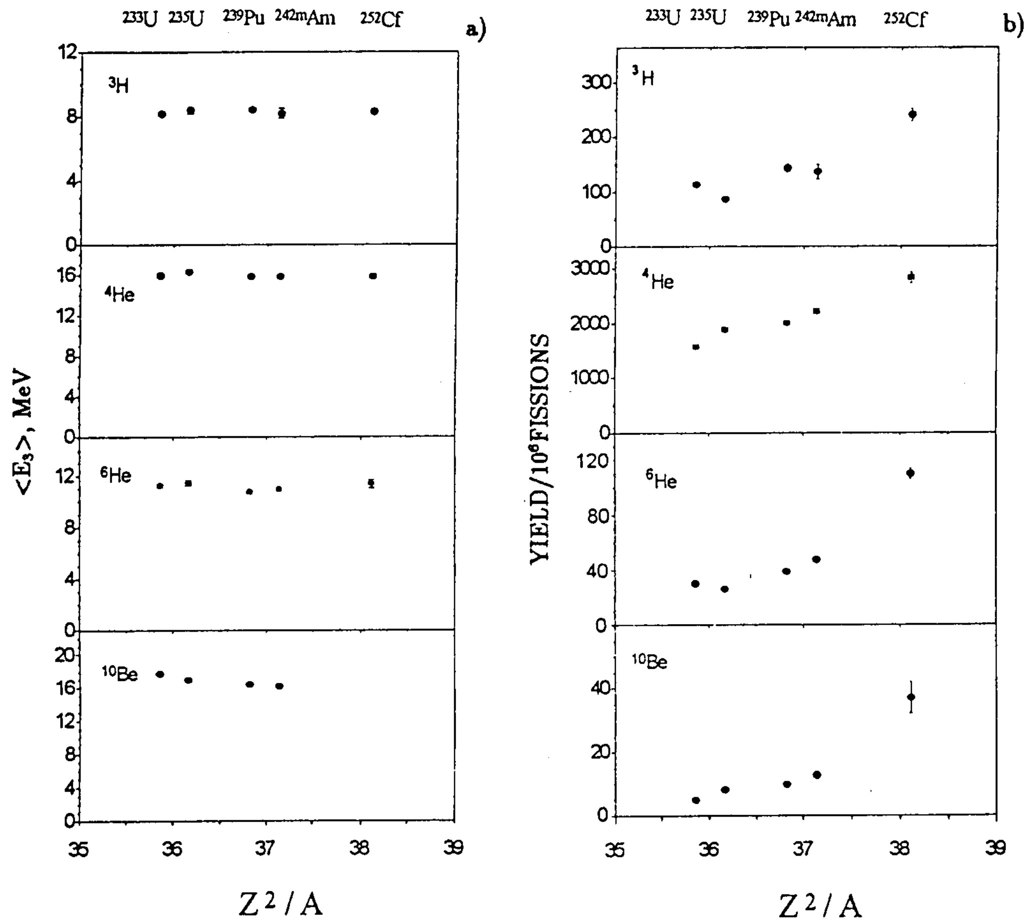

Fig. 3. Dependence of the most probable energies (a) and yields (b) of the light nuclei on Z^2/A of the fissioning nuclei.

The explanation of such behaviour of the energy spectra was given within the framework of the dynamic fission model [4] assuming that the fragments have a considerable kinetic energy E_F^0 at the moment of scission growing with the increase of Z and A of the fissioning nucleus. The light nuclei moving in the fast-changing Coulomb field have no time to realize completely the growing with Z^2/A potential energy into the kinetic energy.

The mass spectra of the light nuclei are characterized by the favoured yields of the M- and Z-even isotopes (^{4,6}He, ^{10}Be, ^{14}C, ^{20}O) with the N/Z ratio close to that of the fissioning nucleus and by the strikingly small yields of the lightest isotopes (^{3}He, ^{6}Li, ^{7}Be, ^{12}C, ^{16}O). The yields of the other isotopes grow with the increase of Z^2/A, the bigger is M (^{6}He, ^{10}Be) the faster is the growth.

The heaviest nucleus identified in our experiment was ^{20}O, with the yield of $Y = (8-16) \times 10^{-8}$ 1/fission. Later in 1989, F.Gönnenwain et al. observed formation of ^{24}Ne on the level of

Positioning of the target close to the reactor active zone in combination with the double focusing magnetic system enabled to obtain high registration sensitivity for light nuclei: 10^{-9}–10^{-8} per fission. The measurements were performed in the two- or three-parametric modes. In the two-parametric mode, the energy spectra of the isotopes ^{1}H, ^{2}H, ^{3}H, ^{4}He, ^{6}He were measured at fixed $B\rho$. In the three-parametric mode, E, T, and $\Delta E/\Delta x$ were measured at $B\rho =$ const. The spectrometer was calibrated with α-particles from ^{244}Cm and with the products of the reaction ^{6}Li$(n,\alpha)^3$H: $E_\alpha = 2.05$ MeV, $E_t = 2.73$ MeV. The spectrometer solid angle remained constant in the whole range of the measured momenta. The registration inefficiency caused by Coulomb scattering and by charge exchange of the ions in the secondary-emission detector (Al_2O_3 film of 5–10 μg/cm^2 thickness) and also by the amplitude threshold in this detector was carefully evaluated. For example, the detection efficiency of ^{10}Be nuclei was known with 10% precision in the E range of 4–40 MeV.

Results of inclusive experiments

All measured energy spectra of the light nuclei are similar in shape. As an example, the energy and mass distributions of the light nuclei from the thermal neutron induced ^{239}Pu fission are shown in Fig. 2. The information on the other fissioning nuclei is given in Refs. [3–6]. The measured most probable energies $< E_3 >$ and the yields Y of ^{3}H and ^{4}He agreed with previous

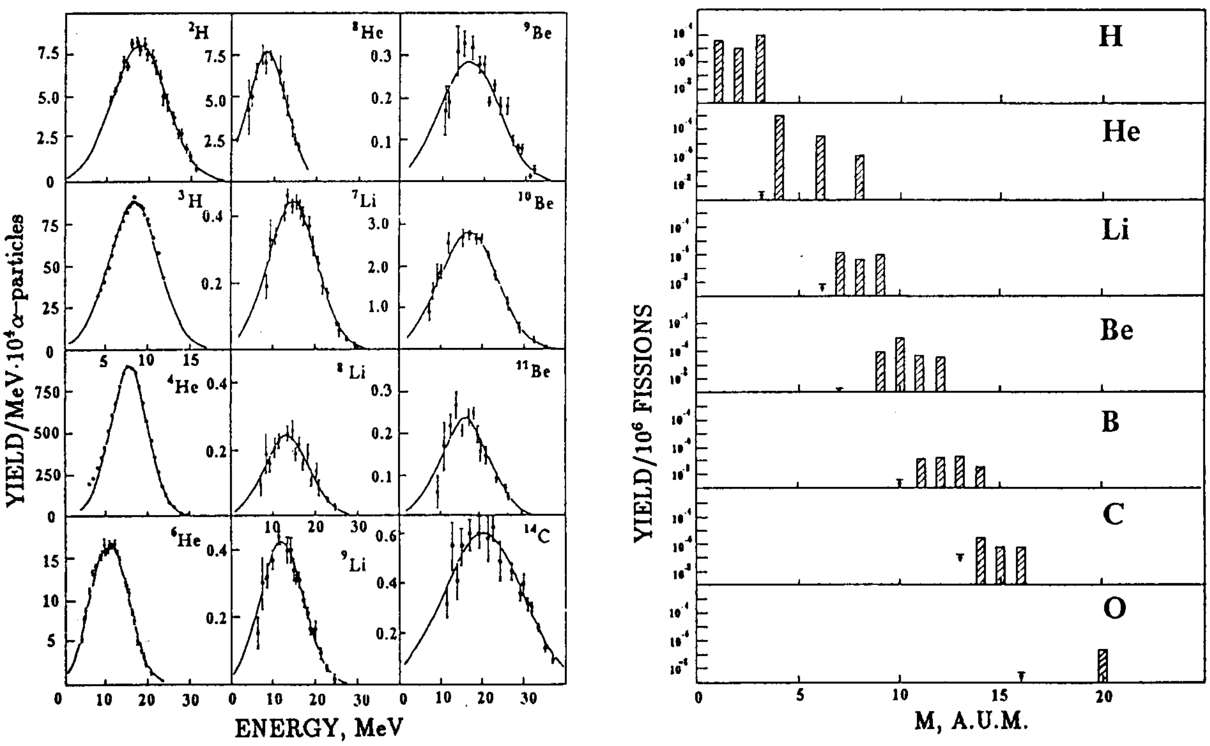

Fig. 2. Energy and mass distributions of light nuclei emitted in fission of ^{239}Pu induced by thermal neutrons. The data are approximated with Gaussian distributions. Arrows point out the upper limits for the yields of the lightest isotopes ^{3}He, ^{6}Li, ^{7}Be, ^{10}B, ^{12}C, ^{16}O.

spectrum shape. The experiments were carried out with different targets – ^{233}U, ^{235}U, ^{239}Pu, ^{242m}Am, exposed to thermal neutron fluxes.

The next stage was the correlation experiments with a special setup which enabled simultaneous detection of the heavy fragments and the light nuclei: ^{3}H, ^{4}He, ^{6}He, ^{10}Be. The detailed studies of the ^{235}U and ^{239}Pu thermal neutron induced fission, as well as spontaneous fission of ^{252}Cf, were performed.

As a result of these studies, a rich experimental material was obtained which created the base for a detailed kinematics analysis aimed at determination of the initial conditions of the fragment separation. Such analysis has been carried out by our group. The main result of the analysis was confirmation of the large value of the fragments initial energy ($E_F^0 \simeq 30$ MeV). This value excluded the statistical model of nuclear fission. Hence, one should look for description of the process on the way indicated by the dynamic model.

Energy spectra and yields of light nuclei measured in inclusive experiments

Experimental method

The measurements of the energy spectra and yields of the light nuclei emitted in the thermal neutron induced fission of ^{233}U, ^{235}U, ^{239}Pu, ^{242m}Am were carried out with the magnetic time-of-flight mass-spectrometer [1,2] installed at the WWR-M neutron reactor. The scheme of the spectrometer is shown in Fig. 1.

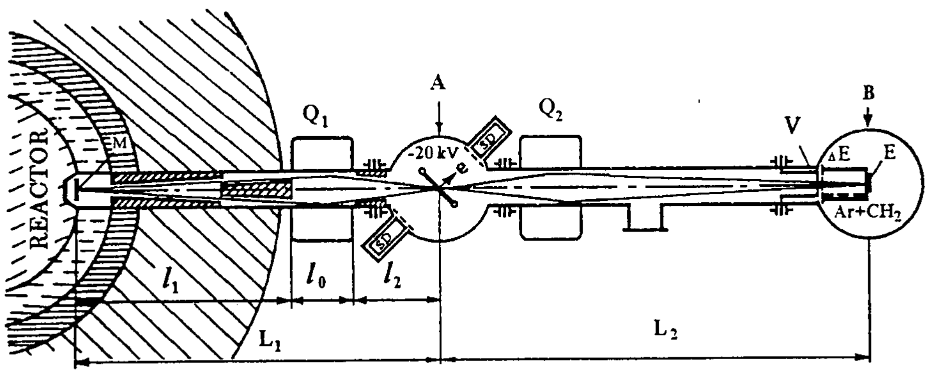

Fig. 1. Scheme of the magnetic time-of-flight mass-spectrometer. M – target of fission material, Q_1 and Q_2 – doublets of quadrupole lenses, SD – scintillation detectors of secondary emission electrons, V – vacuum-tight window 50 $\mu g/cm^2$ thick, E – silicon detector, ΔE – gridded ionization chamber at 50–200 torr pressure.
$l_1 = 3.5$ m, $l_0 = 0.8$ m, $l_2 = 1.7$ m, $L_1 = 6$ m, $L_2 = 7.5$ m.

Identification of the charged particles according to their mass M and charge Z was done via simultaneous measuring of the particle magnetic rigidity $B\rho$, the energy E, the specific ionization $\Delta E/\Delta x$, and the time-of-flight T on the base L_2. The range of identifiable isotopes was $1 \leq Z \leq 8$ and $1 \leq M \leq 20$ where the upper limit was determined by the real yield of the light nuclei. In the energy range of 5 MeV to 30 MeV, the mass resolution was $\Delta M/M = 1$–2%.

TERNARY FISSION

A.A.Vorobyov, D.M.Seliverstov

Introduction

In this paper we briefly describe a series of experiments on ternary nuclear fission performed at the Gatchina WWR-M neutron reactor in the period from 1966 to 1987. Two alternative approaches in description of the nuclear fission process were widely discussed in the 60s. Within the framework of the statistical fission model (P.Fong, 1956), descending from the saddle point was considered to be adiabatically slow (large viscosity of the nuclear matter), so formation of the fragments occurs just before the scission point. On the contrary, in the dynamic model of fission (I.Halpern, 1963) the formation of the fission fragments takes place at the barrier, and further separation of the fragments goes so rapidly (small viscosity of the nuclear matter) that no significant redistribution of the fragment masses occurs. It would be possible to distinguish these hypotheses having measured the kinetic energies of the fragments E_F^0 immediately in the moment of the fragment separation ($E_F^0 \sim 1$ MeV in the statistical model and $E_F^0 \geq 20$ MeV in the dynamic model). Unfortunately, the E_F^0 value cannot be determined in the usual fission into two fragments because the measured energy of the fragments is the sum $E_F = E_F^0 + V_C$, where V_C is the potential Coulomb energy of the fragments in the moment of separation. These terms are not measured separately. Having this in mind, it seemed promising to include into consideration the ternary fission, that is the fission with emission of α-particles and other light nuclei, as the energy and angular distributions of the emitted particles must depend on the initial velocities of all the three fragments.

The fission with α-particle emission discovered by L.Alvarez in 1944 was further studied in the 60s by photo-emulsion (Z.I.Solovyov and R.A.Filov) and electronics (S.S.Kovalenko et al.) methods at the Radium Institute (Leningrad). The first publication showing that not only α-particles but also some other light nuclei are formed in the process of ternary fission appeared in 1967 (S.Cosper et al.). The first kinematics calculations of the ternary fission were carried out by B.G.Geylickman and G.I.Khlebnikov in 1965. Much more advanced calculations were performed by Z.Fraenkel et al. in 1967 with description of the correlation data on α-emission in the ^{252}Cf fission. These calculations demonstrated better agreement with the experimental data while using large value of $E_F^0 \approx 40$ MeV. But this consideration was not conclusive in view of the incompleteness and low accuracy of the experimental data and because of the model dependence of the calculations.

In 1966 our group has constructed a multi-parameter spectrometer for measuring the inclusive spectra of light nuclei formed in the ternary fission. The distinctive features of the spectrometer were:

- High sensitivity – light nuclei with the yields down to 10^{-9} per fission were registered.
- High mass resolution for light nuclei – $\Delta M/M$ = 1–2%.
- Low energy threshold – practically no absorption materials on the path of the particles.

With the help of this spectrometer, we extended significantly the variety of detected light nuclei: ^{2,3}H, ^{4,6,8}He, ^{7,8,9}Li, ^{9,10,11}Be, ^{11,12,13,14}B, ^{14,15,16}C, ^{20}O. Also, we were able to measure the energy spectra of light nuclei down to small energies and thus to determine reliably the